Chapter 2 Satellite image analysis

2-1 Data processing and generation of image

2-1-1 Data used for the analysis

For use in analyzing geology and geological structure and extracting alteration zone of the survey area, false color images and ratio image of 13 scenes were prepared. In addition, false color and ratio digital mosaic images and covering the whole area were produced. Most of the data used for the images were observed by the Landsat 5 (data for Path 231/Row 91 by Landsat 4) and stored in bulk-corrected CCT's (computer-compatible magnetic tapes) that were purchased from the U.S. EROS Data Center through the Remote Sensing Technology Center. Location of the images of 13 scenes is shown in Fig. II-2-1, and observation data such as date of acquisition, sun position, etc. are given in Table II-2-1.

Table II-2-1 Path/Row, date of acquisition, sun azimuth and sun elevation of the Landsat TM image of 13 scenes (areas)

No.	Name of the scene (area)	Path	Row	Date of acquisition	Sun azimuth	Sun elevation
1	Malargue	232	85	Feb. 9, 1987	75°	44°
2	Chos Malal	232	86	Feb. 9, 1987	74°	44°
3	Zapala	232	87	Feb. 9, 1987	73°	43°
4	San Martin de Los Andes	232	88	Feb. 9, 1987	72°	42°
5	San Carlos de Bariloche	232	89	Feb. 22, 1986	65°	40°
6	Lago Menendez	232	90	Dec. 7, 1986	73°	50°
7	Plaza Huincul	231	87	Jan. 1, 1987	80°	50°
8	Laguna Blanca	231	88	Oct. 29, 1986	63°	46°
9	Ojo de Agua	231	89	Oct. 29, 1986	62°	45°
10	Esquel	231	90	Jan. 27, 1985	71°	46°
11	Senguerr	231	91	Feb. 24, 1992	68°	34°
12	Colelache	230	90	Dec. 9, 1986	73°	50°
13	Buen Pasto	230	91	Dec. 9, 1986	72°	49°

Before purchasing the data, condition of acquiring Landsat TM data covering the survey area and its availability was first inquired to the U.S. EROS Data Center through the Remote Sensing Technology Center. The best data for image analysis was selected in consideration of data deficiency, the amount of clouds and snow, and the time of observation. For naming the image a representative local name of the area for each image was employed, and serial numbers were given from the northwestern end to the southeastern end.

In the preparation of false color and ratio images a method was developed by which the same lithofacies and the same alteration zones can be expressed in the same color tone, even though scenes to which they belong are different. Also, by the same band combination with

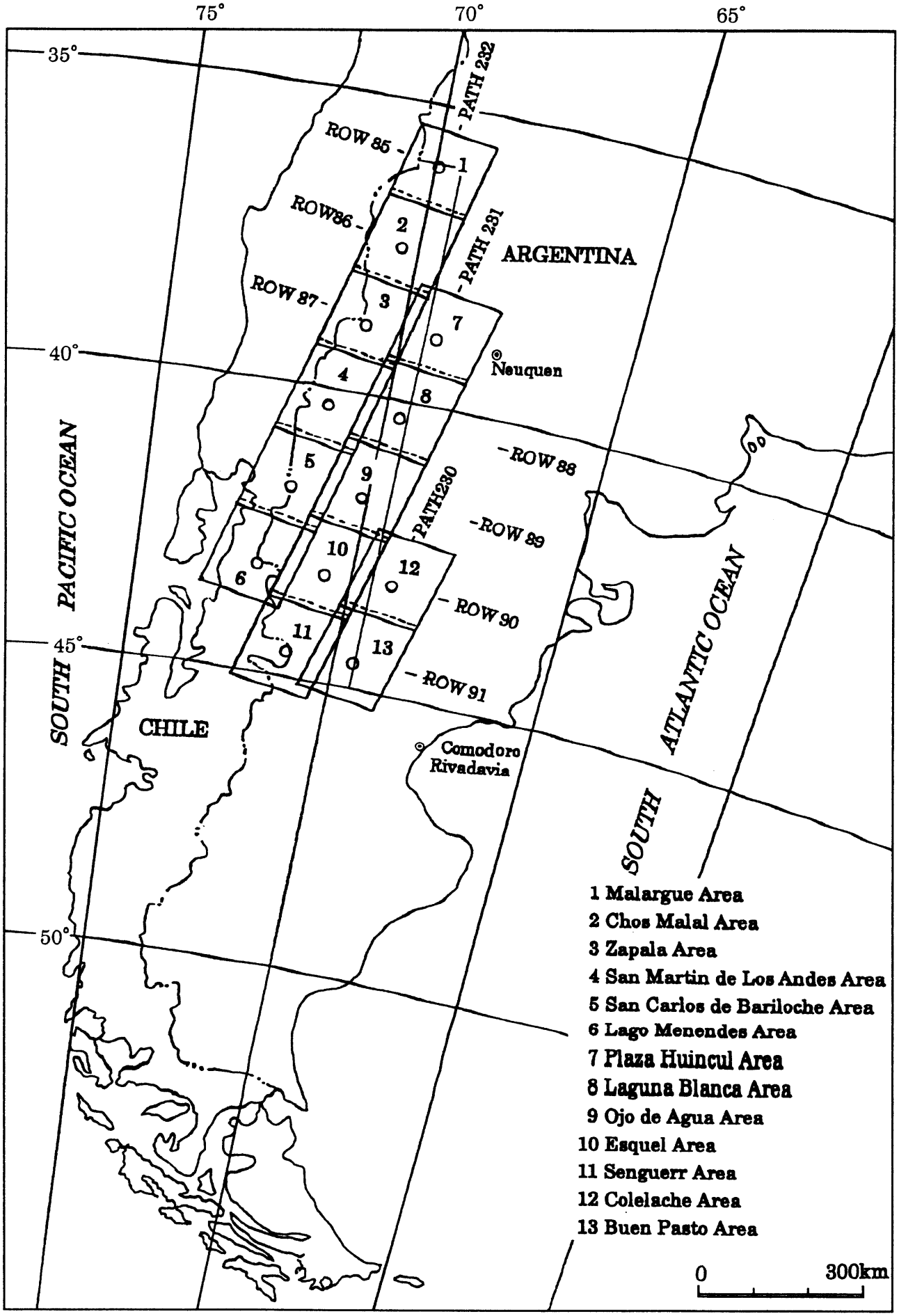

Fig. Ⅱ-2-1 Index map of 13 scenes of Landsat TM image over the survey area

the false color images of 13 scenes, a digital mosaic image covering the whole area were prepared. When preparing a mosaic image, attention was paid not to producing different color tone between adjacent images. Method of producing images described below.

2-1-2 Generation of false color synthetic images

Before producing false color synthetic images correction of radiant quantity is required which includes corrections of incident light quantity, atmospherie and directional reflection coefficient. Reasons for the corection and its method are described as follows:

(1) Reason for the correction of radiant quantity

For ranges of wavelength observed by the TM (Thematic Mapper) sensor on board Landsat there are four bands in the visible to near-infrared, two bands in the shortwave-infrared, and one band in the heat-infrared range totaling seven bands. The observed analog image data are converted into 256 gradations of digital values from 0 to 255 for each pixel.

Luminance obtained by an optical sensor such as Landsat TM reflects reflection of sunlight from the earth surface in the visible to near-infrared range, and thus makes it possible to discern surface objects by the difference in spectral reflectance inherent to each object. The spectral radiance incoming to the satellite sensor is a result of the process that sunlight is reflected on the surface and passes through the atmospheric layers. Therefore, in addition to the reflected light from the earth, the radiance reaching the satellite sensor includes radiant and scattered lights emitted from the atmosphere called pass radiance and the scattered radiation called sky light which scatters in the atmosphere and are incident from all the directions. Accordingly, the spectral radiance obtained by the sensor observing just underneath at wavelength of λ can be approximated by the following equation:

$$L(\lambda_1, \lambda_2)=\int_{\lambda 2}^{\lambda 1} K(\lambda)[\tau a(\lambda)\{U(\lambda)+P(\lambda)\}\rho(\lambda)+b(\lambda)]d\lambda$$

where,

$L(\lambda_1, \lambda_2)$: Spectral radiance input to the sensor over wavelengths λ_1 to λ_2

$K(\lambda)$: Response characteristic of the sensor

$\tau a(\lambda)$: Atmospheric transmittance of reflected light.

$U(\lambda)$: Radiance of direct sunlight

$\rho(\lambda)$: Surface reflectance

$b(\lambda)$: Atmospheric radiation and scattered light between the sensor and the object.

$P(\lambda)$: Radiance of sky light, that is the downward scattering sunlight.

Of the above, b (λ) becomes the additive element of luminance, and U (λ), P (λ) and τ a (λ) are the multiplicative elements. Because the effects of these elements are different depending on the quantities of steam and aerosol in the atmosphere, the same values are not obtained on the same material if the observations are conducted at different times. Also, the effect of these absorbed light and scattered light is dependent on the wavelength, so that the band ratio of spectral reflectance of a material does not have a fixed value in images acquired at different times. Consequently, if images are processed with the radiant quantities of each band uncorrected, the same material is expressed in different color tones, and the comparison and discrimination of materials become impossible.

Because the image data used for this survey were acquired in different times, the correction of radiant quantities was made on the basis of the following assumptions in order to express the same material in the same color tone in all the images:

- Response characteristics of the sensor is output in a primary linear form (i.e., $y = ax$) to the incident luminance.
- The atmospheric transmittance of reflected light is equal in any area within an image.
- The atmospheric radiation and scattering between the sensor and the object are equal in any area within an image.
- The sky light radiance is equal in any area within an image.

(2) Correction of incident light quantity

The radiance of direct solar radiation that is incident on a unit area differs from location to location even within an image. For example, in the southern hemisphere where the sun radiates from the north, the direct solar radiation incident on a unit area within an image is larger in the north and smaller in the south. Hence, the incident light was corrected and the sun elevation was fixed at 60° from the geographical coordinate position of each pixel, the sun azimuth and elevation given to the image.

(3) Atmospheric correction

Atmospheric correction is the correction of τ a (λ) and b (λ). This correction requires the values of incident light quantity {U (λ) + P (λ)} and surface reflectance ρ (λ).

The correction of incident light quantity described in (2) assumes that all the objects within an image are flat. In reality, however, there is topographic relief which gives different values of {U(λ) + P (λ)} for the same location in images acquired at different times because of a difference in the solar position. The use of a high-precision DTM (digital terrane model) to correct the {U λ) + P (λ)} may be one solution to this problem. This solution, however, does

not seem realistic because areas to which high-precision DTM can be applied are limited. Consequently, a method was employed to use numerous corresponding pixels between two images and to statistically process overlapped areas to eliminate dependency on topographic relief.

A method generally employed is to make average luminance and standard deviation coincident using statistics of the entire overlapped areas.

$$P'_{ij}=(P_{ij}-P_{av})/\sigma_p \times \sigma_q+Q_{av}$$

where,

P_{ij}': Conversion value of brightness

P_{ij}: An arbitrary point of an image converted for luminance

P_{sv}: Average luminance of an image converted for luminance

Q_{av}: Average luminance of a standard image

σ_p: Standard deviation of luminance of an image converted for luminance

σ_q : Standard deviation of luminance of a standard image

In this case, it is assumed that there are virtually no significant changes in the surface material in an overlapped part of image and that $\rho(\lambda)$ on two observation times are equal. However, in images which were acquired on different occasions (seasons), vegetation, amount of snow and clouds, mist, lake and river channels, and surface structures should change in the overlapped part. Therefore a method using average luminance and standard deviation cannot be applied. Because many changes in the surface material were found in overlapped part of the images, the following method was used in this analysis:

For all the corresponding points within the overlapped image, luminance of a standard image was taken on the axis of abscissa and that of a corresponding image on the axis of ordinate, and then difference of luminances between the corresponding points was analyzed. Such differences, if drawn on a scatter diagram, will be easy to discriminate, because distribution of corresponding points such as vegetation, shadow, snow and clouds whose spectral reflectance $\rho(\lambda)$ changes significantly become a random or significant point groups.

In most of the corresponding points eliminating them, there is no large change in $\rho(\lambda)$, and the point groups scatters along a certain straight line with high correlation. The distribution of such an extension reflects the difference of $\{U(\lambda)+P(\lambda)\}$ due to topographic relief. Therefore, topographic effects were eliminated by a primary regression using the least square method.

From the corrected primary regression equations $\{U(\lambda)+P(\lambda)\}$ and $\rho(\lambda)$ obtained with the above method, the atmospheric correction coefficient can be calculated based on $\tau a(\lambda)$ and $b(\lambda)$ between the two images. This primary regression equation, if observations are

made on one day, can be approximated to a straight line passing through the origin. This means that the atmospheric transmittance $\tau a(\lambda)$, atmospheric radiation and scattered light $b(\lambda)$ between the two images are the same.

For images on different observation dates, this primary regression equation can be generally expressed by $y = ax + b$, which does not pass through the origin. This shows that the atmospheric transmittance $\tau a(\lambda)$, atmospheric radiation and scattered light $b(\lambda)$ between the two images are not the same. The regression equation enables the atmospheric transmittance $\tau a(\lambda)$, atmospheric radiation and scattered light $b(\lambda)$ between the two images to be identical.

To be more accurate, these terms are the values to be obtained by multiplying $\tau a(\lambda)$ and $b(\lambda)$ by $K(\lambda)$, as gain of a sensor is different when the data are obtained. In this method, however, gain of a sensor can also be corrected simultaneously.

Because the atmospheric correction between observations on the same day has higher precision, the atmospheric correction of all the 13 scenes was executed according to the following procedures;

(a) Atmospheric correction is conducted for each path, so that the northern end of each path is determined to be a reference image.
(b) Atmospheric correction of each image is proceeded southward one by one along a path.
(c) The central path (P231) was a reference for atmospheric correction among the three paths.

By undergoing these processes, it becomes possible to make the atmospheric conditions of the entire image agree with those of the central north end image (P231/R087).

(4) Correction of directional reflection coefficient

In a perfect diffusion reflective material, let's define that the reflective coefficient of reflected light that is vertically incident on the material and vertically observed is 1. If the observation position is changed from vertical to horizontal, the reflective coefficient gradually decreases from 1 to 0.

Each image of LANDSAT TM has a transverse (roughly E-W direction) angle of visibility of about 16°. This results in an angular difference of about 16° between the right and left sides of an image for an angle formed by the sun-the observed materials-the observer, when the sunlight radiates from the right side of the image. In such a case, a similar phenomenon as observing a perfect diffusion reflective material from a different angle will occur. Because this directional reflection coefficient varies by materials and wavelengths, and is dependent on

topography, it is impossible to correct it for each pixel. If the eastern end and the western end of an image are compared within the image (based on assumptions that the sun radiates from the east at azimuth of 90° and elevation of 60°, that there is no relief on the surface, and that the same materials as basalt on the moon occur), however, luminance is reduced by about 10% on the right (eastern) side where an angle formed by the sun-the observed material-the observer becomes larger. When three images are stitched from east to west and luminance is 1 of the western end of the adjoined image, this causes luminance reduction of about 27% ($=0.9^3$) at the eastern end and makes the eastern side obviously darker.

Therefore we have examined how luminance changed over the whole image by the use of statistics based on the atmospherically corrected images. The reason why statistics was employed is to remove effects from surface relief and different surface materials. For the statistic of each column some 3,000 to 10,000 data were used. Luminance value of each pixel is expressed as a matrix, and average and standard deviation of each line and column were calculated. Because each image is a parallelogram, a position where image was first acquired at the western end was shifted laterally to make a matrix whose acquisition positions are aligned.

The upper figure of Fig. II-2-2 shows horizontally (in the E/W direction) the variation of arithmetical averages obtained along the column (in the N/S direction). The axis of ordinate expresses the ratio of variation with the average of each band to be 1. This figure shows three scenes (P232 to 230) from east to west with an apparent reduction of luminance in the eastern part of the image. In the analysis carried out so far in by the survey in the eastern Andes area of Argentine, about 7% reduction of luminance was observed in the eastern part of a scene. By applying this factor to the present analysis and compensating the reduced luminance by 7% per scene, a generally flat curve of average luminance was obtained except for the left end area covered with snow and sea and the right part where sufficient data were not available.

(5) Preparation of false color image

By means of the radiation quantity correction method described above, the luminance of all the scenes were unified to the reference luminance of P231/R087. The statistics (average, standard deviation and distortion) of Landsat TM image data is different for each band, and data scattering is generally small, that is a range of 20 to 30 (256 gradations). Consequently, the use of such data would produce images of unacceptable color balance, small data scattering, and small difference in color tone, which therefore would not be adequate for image interpretation.

In order to solve these problems so that the radiation quantity correction images of all the scenes can be appropriately produced, the same luminance correction was conducted for all the scenes using the non-linear stretch. This correction was non-linear stretching to attain

a distribution close to the normal distribution having an average luminance of about 115 (256 gradations: the same gradation difference is easier to discriminate in a darker area). The normal distribution was calculated so that 2.5 times the standard deviation would correspond to 115 gradations. The statistics of the entire area was calculated by avoiding areas covered with cloud, snow and water.

For image enhancement, there are various methods including the Laplacian, Gaussian filters and local enhancement processes. The Gaussian filters and local sharpening processes, however, employ stretching methods variant from field to field to emphasize difference from the surrounding materials. As a result, even the same material could be shown in different color tones if it is placed in different fields. Hence, the present image enhancement process employed only the Laplacian filters to avoid such a phenomenon.

For the combination of the band of false color image, combination of Band 1, 4 and 5, Band 1, 4 and 7, and Band 4, 5 and 7 were examined. Intermediate volcanic rocks widely occur in the survey area, and the combination of Band 1,4 and 5 is suitable to interpret geological structure of intermediate volcanic rocks. Therefore, an image was produced by allocating the colors of blue, green and red to Band 1, 4 and 5, respectively.

(6) Geometric correction

The images were converted geometrically into the UTM coordinate using the produced false color images and topographic maps (scale: 1/500,000). It was difficult to select high-precision GCPs (Ground Control Points), because the most precise topographical map which was available was 1/500,000 in scale and most of the survey area consists of mountains and deserts which do not include markers such as a river. Then, river junctions and road crossings were used as GCPs and 15 to 20 points were selected per image. Pseudo Affine Conversion was used for interpolation and low-precision GCPs were deleted so that the error from the result of the least square method should be less than 30 pixels (about 1 km).

An error less than 30 pixels corresponds to about 2 mm in a 1:500,000 topographical map, which is near the limit of geometric correction when the precision of the topographic map and the conditions of survey area are taken into consideration. It should be noted that the first order extrapolation method was used for geometric conversion and re-sampling was carried out with a size of 30 m per pixels.

2-1-3 Preparation of ratio image

(1) Principle of ratio image

Landsat TM observes spectral radiance input into the sensor in seven bands of wavelength which range in visible to near-infrared and intermediate-infrared. The radiance

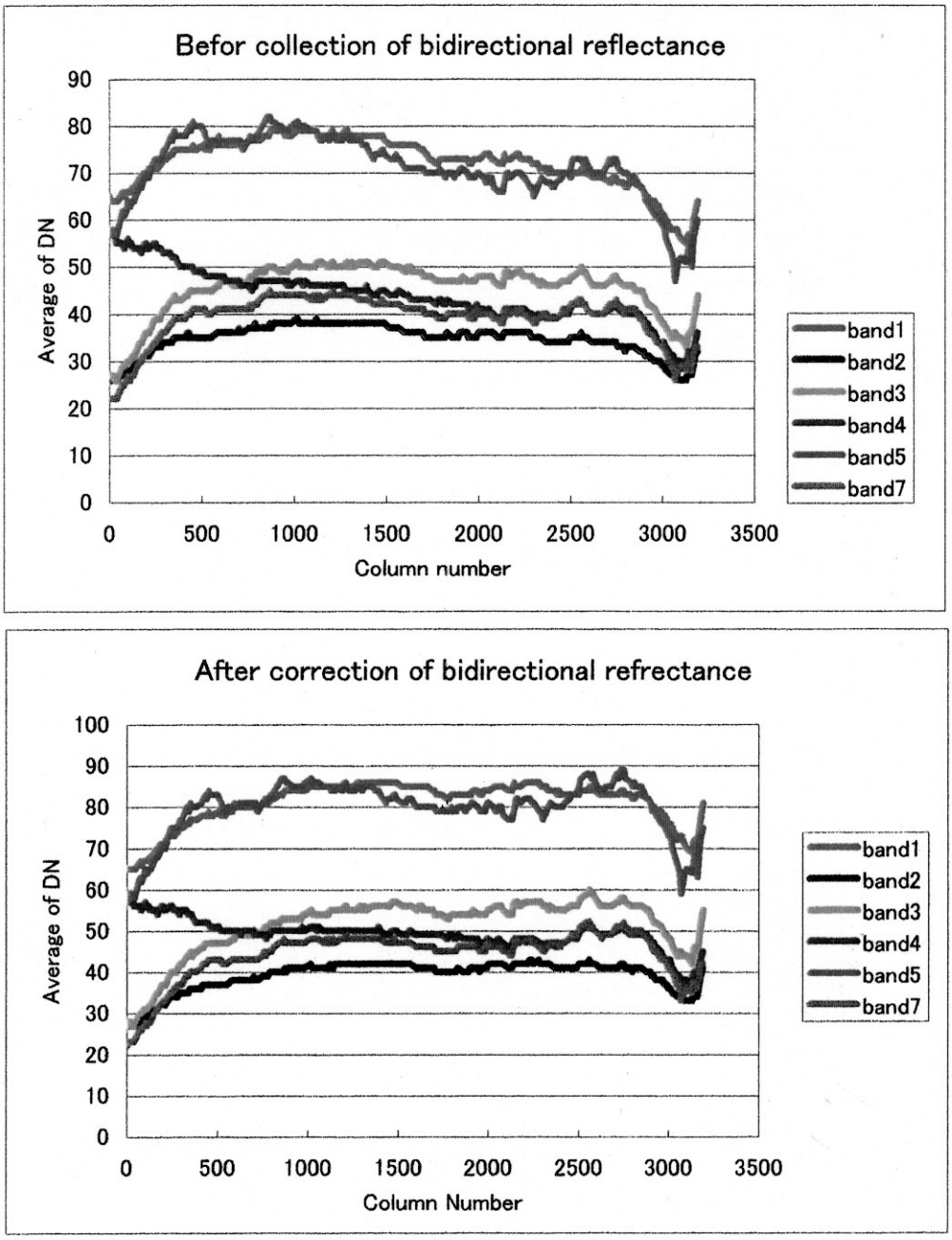

Fig. Ⅱ-2-2 Lateral variation of the brightness due to directional reflectance
(vertical axis: Average of digital number of brightness
horizontal axis: Column number of lateral pixel)

of an earth material , N_1 (unit: $mW/cm^2{}_{SK}$), when observed by the sensor can be expressed by the following equation:

$$N_i=(1/\pi)(H_iR_iT_iA_i)+N_{pi}$$

where,

H: Sun light irradiance

R: Reflectance of an earth material

T: Atmospheric transmission coefficient (vertical).

A: Coefficient determined by both angles formed by a line conecting the sun, the earth material and the surface and formed by an earth material and the sensor.

N_p: Atmospheric path radiance.

i: Band of the sensor

Because, if N_p is assumed, A becomes constant regardless of the channel, and H and T take fixed values by each channel, the spectral characteristic can be emphasized by the ratio between the two channels. When looking into the ratio between channels of maximum and minimum values in the reflective spectral pattern of a mineral, an mineral-containing pixel makes the ratio larger and it becomes easier to discriminate it from a pixel where no minerals occur. The basic idea of processing for ratio image is to apply this characteristics to the emphatic presentation of an area of a certain mineral distribution in the image.

The processing for ratio image places the minimum digital value as the atmospheric path radiance, obtains the value by subtracting the minimum value from the digital value of each band, and obtains the ratio between these bands. The ratio between the bands is usually in a range of 0 to 10, but density conversion as described in Chapter 2-1-2 (Production of false color synthetic image) is necessary to express the ratio between bands in the image. The following procedures were employed for conversion of brightness:

Referring to the known alteration zones recorded in the existing geological data, the distribution of ratio values was obtained for the alteration zones. Slightly larger value than this distribution was defined, and pixels having its ratio values outside this scope were given the value of 0. Except for the ratio values of 0, the scattering of the rest of the ratio values was smaller than the scattering of the original ratio values. Thus, the conversion of brightness made the presentation with a variety of brightness possible. The conversion of brightness is expressed by the following linear function:

$$G_i=a \cdot F_i+b$$

where,

G_I: Density of output image. a: Gain.

F_I: Value of color-ratio processing. b : Bias.

a and b are obtained from the distribution of actual values of color-ratio processing.

(2) Generation of images

Porphyry copper deposits and epithermal gold deposits are distributed in the survey area, accompanied by the inherent hydrothermal alteration zones. The validity of the band ratio 5/7, 4/5 and 3/1 for the extraction of these hydrothermal alteration zones from the Landsat TM data has been proved by the past work in the Escondida area and the Belgua Progreso area in Chile.

In the present survey, in areas of P232/R085 and P232/R086 where known alteration zones are present, ratio images were compared by a combination of the band ratio 5/7, 4/5 and 3/1 and the other combination of 5/7, 4/7 and 4/5. As a result, it was found that the most effective for the extraction of alteration zones was a combination of the band ratio 3/1, 4/5 and 5/7 allocated to B, G and R. In this combination of the band ratio, the alteration zones are shown in reddish pink and whitish pink colors. In the ratio image of the other areas, the average of gain and bias that became the best in the two areas was used.

(3) Principal component analysis

From its nature, the ratio image makes it possible to eliminate shadows caused by topography. On the other hand, loss of topographic features makes identification of the area difficult. Hence, to make identification of the area easier, the present survey produced ratio images with topographic information.

A few methods are available to express topographic features; one is the use of Band 5 which reflects topographic features, and the other is the use of the first primary component in the analysis of main components which is considered to reflect topographic information. In this survey, the first primary component in the analysis of main components was employed.

The contribution rate of each band to the first primary component in each image was in a range of 0.37 to 0.43 and the difference in the contribution rate between the images of each band was very small. Hence, the average contribution rate of each band was calculated and it becomes the contribution rate to the first primary component.

For the topographic information, the contribution rate was multiplied for each band and appropriate gain and bias were set to the summed up value (the average of the total becomes 0), and they became the topographic information coefficient. Then, the topographic

information coefficient was multiplied to the luminance of the ratio image prepared in (2). It was the ratio image which is accompanied with topographic information.

For geometric correction, the same GCP as that used for the geometric correction in the production of false color synthetic image (Section 2-1-2) was used, and geometric conversion to the UTM coordinate system was executed by the same method.

2-1-4 Preparation of mosaic images

(1) Image compression and geometric conversion

In order to create a 13-scene false color mosaic image, image compression was conducted to reduce the image size. The reason for proceeding compression is that the mosaic image without compression would be voluminous, comprising 17,000 pixels by 41,000 pixels by 6 bands = 4.2 GB, and the data would exceed the physical limit of film output.

From the image of each scene in which the radiant quantity was corrected, compression was made by the geometric conversion of the first order extrapolation method, and 16 pixels (4 x 4) were reduced to one pixel. Then, from overlapping area of the two images 10 to 20 corresponding points were visually selected and the geometric conversion coefficient was calculated by Helmert's conversion using the least square method. In this process, the coefficient of Helmert's conversion was obtained by eliminating data of larger errors so that errors after re-calculation shall be not more than one picture element. Geometric conversion was done by the use of the first order extrapolation method.

(2) Stitching images

Images acquired at different occasions have areas with apparently different color tones in the stitched part between two images attributable to changes in surface covers, position of shadows and clouds. Even though this apparent change in color tone does not interfere geological interpretation, it will give an impression of imperfection to producing and refining mosaic images. To improve this insufficiency, a "staggering image stitching method" was newly developed in which areas of smaller tonal difference were searched for stitching images. In this method if there is an area that has clouds or in which shadow position changes in an image, stitching can be conducted detouring the area.

Images were stitched one by one starting from the northernmost image of each path, and three oblong mosaic images of P232/R085 to P232/R090, P231/R087 to P231/R091 and P230/R090 to P231/R091 were produced. Then, with a mosaic image of P231 as a reference, corresponding points on the image on either side were chosen. The images were stitched by the above method after geometric conversion by Helmert' s conversion. Size of image produced by joining three paths was about 4,400 pixels by 10,200 pixels.